

Hot Paper

Polyhedral Oligomeric Silsesquioxane D_{3h} - $(\text{RSiO}_{1.5})_{14}$ Marc Hunsicker,^[a] Ankur,^[a] Bernd Morgenstern,^[b] Michael Zimmer,^[a] and David Scheschkewitz*^[a]

Dedicated to the memories of Robert West and Petey Young

While smaller polyhedral oligomeric silsesquioxanes T_nR_n (POSS) are readily accessible or even commercially available, unambiguously authenticated larger systems ($n > 12$) have barely been reported. Synthesis and isolation procedures are lengthy, and yields are often very low. Herein, we present the surprisingly straightforward and high-yielding access to the phenyl-substituted derivative of a so far only postulated second D_{3h} -symmetric T_{14} isomer and with that the largest crystallographically characterized POSS cage with organic substituents.

Treatment of the commercially available incompletely condensed $T_7\text{Ph}_7(\text{OH})_3$ silsesquioxane with catalytic amounts of trifluoromethanesulfonic acid results in high yields of the $T_{14}\text{Ph}_{14}$ framework, which is isolated in crystalline form by a simple work-up. D_{3h} - $T_{14}\text{Ph}_{14}$ was analyzed by single crystal X-ray diffraction, multinuclear NMR spectroscopy and thermal analysis. The relative energies of all four theoretically possible $T_{14}\text{Ph}_{14}$ isomers were determined by optimization of the corresponding structure using DFT methods.

Introduction

Silsesquioxanes $[\text{RSiO}_{1.5}]_n$ are polymeric or oligomeric materials with a wide variety of applications in materials chemistry, e.g. as building blocks in inorganic-organic copolymers and other hybrid materials,^[1a] precursors for silicon nanocrystals,^[1b] electron beam resists,^[1c] chemical sensors,^[1d] and as model systems for silicon surfaces.^[2] Many oligomeric silsesquioxanes adopt cage-like molecular structures (polyhedral oligomeric silsesquioxanes POSS, $R = \text{H}$, alkyl, aryl). Their high stability gives rise to a broad range of further manipulations in the POSS framework periphery.^[3] The common abbreviation T_nR_n refers to the number n of trifunctional silicon centers T each carrying a single substituent R . Early synthetic procedures^[4a-c] employed the controlled hydrolysis of trihalo- or trialkoxysilanes followed by the condensation to often complicated mixtures of variously sized molecular cages as well as polymers. Long reaction times, low yields and tedious separation procedures limited the potential applications initially. The use of NBu_4F as catalyst improved yields in case of T_8R_8 significantly (Figure 1, A) despite

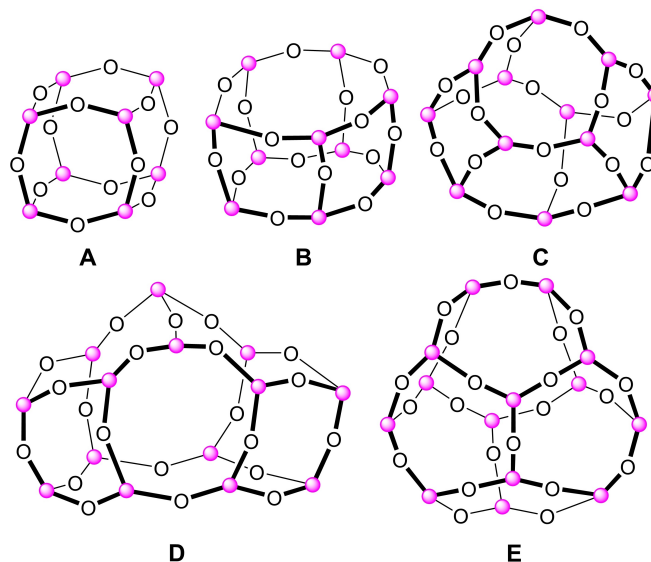


Figure 1. Exemplary POSS derivatives characterized in the solid state by X-ray crystallography. A: T_8R_8 ; B: $T_{10}R_{10}$; C: D_{2d} isomer of $T_{12}H_{12}$; D: D_{3h} isomer of $T_{14}H_{14}$; E: C_{2v} isomer of $T_{14}H_{14}$ (● = SiR).

[a] M. Hunsicker, Ankur, Dr. M. Zimmer, Prof. Dr. D. Scheschkewitz
Krupp-Chair of General and Inorganic Chemistry
Saarland University
66123 Saarbrücken, Germany
E-mail: scheschkewitz@mx.uni-saarland.de

[b] Dr. B. Morgenstern
Service Center X-Ray Diffraction
Saarland University
66123 Saarbrücken, Germany

Supporting information for this article is available on the WWW under <https://doi.org/10.1002/chem.202303640>

© 2023 The Authors. Chemistry - A European Journal published by Wiley-VCH GmbH. This is an open access article under the terms of the Creative Commons Attribution Non-Commercial NoDerivs License, which permits use and distribution in any medium, provided the original work is properly cited, the use is non-commercial and no modifications or adaptations are made.

much shorter reaction times.^[4e] A large number of T_8R_8 derivatives have thus been crystallographically characterized, as well as a few examples of the larger cages $T_{10}R_{10}$ (B) and $T_{12}R_{12}$ (C).^[5] The largest POSS cages with unambiguously determined solid state structure are two of the four possible $T_{14}H_{14}$ isomers with D_{3h} and C_{2v} symmetry (D and E).^[4c,6] Recently, a styryl-functionalized $T_{18}R_{18}$ isomer was isolated in low yield from a complex product mixture, but its structural characterization was restricted to spectroscopic observations and DFT calculations.^[7] Using larger silsesquioxane cages as precursors for materials may lead to altered, possibly improved properties, for example in hybrid porous polymers and materials with low dielectric constants.^[8]

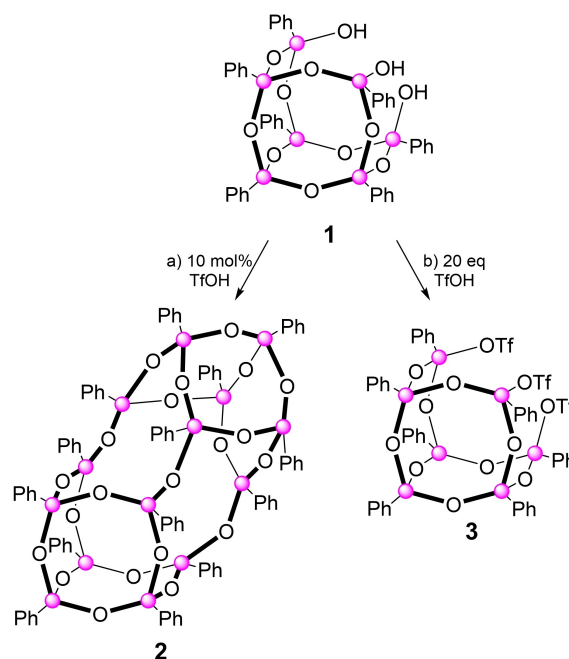
Herein, we report the simple and systematic preparation of one of the two elusive T_{14} framework isomers as crystalline material. With its phenyl-substituents, the obtained $T_{14}Ph_{14}$ represents the largest organic POSS derivative with unambiguously determined solid state structure to date. Its straightforward and reliable high yield synthesis by condensation of the commercially available trisilanol $T_7Ph_7(OH)_3$ is enabled by the catalytic action of trifluoromethanesulfonic acid (TfOH). We also obtained circumstantial evidence for the formation of triflates of the type $T_7Ph_7(OTf)_n(OH)_{3-n}$ under closely related reaction conditions.

Results and Discussion

Given the resemblance of the commercially available trisilanol $T_7Ph_7(OH)_3$ to one half of the postulated, yet experimentally elusive second D_{3h} isomer in the $T_{14}H_{14}$ system, we speculated that a condensation reaction may result in an analogous $T_{14}R_{14}$ structure. Pietschnig et al. previously reported that the corresponding *tert*-butyl-substituted $T_7^tBu_7(OH)_3$ forms a dimer in which two T_7 units are connected by hydrogen bonding through the silanol groups.^[9] Thermal rearrangement above 200 °C was postulated to form the aforementioned second D_{3h} $T_{14}R_{14}$ isomer among other possible condensation products, based on MALDI-TOF-MS data.^[10] As spontaneous self-condensation at ambient temperature does apparently not occur in either case, and considering the NBu_4F catalyzed condensation of silanetriols towards T_8R_8 silsesquioxane frameworks,^[11] we concluded that a catalyst would be required in order to enable a nucleophilic attack of the OH groups of one molecule at the open face of a second.

Trifluoromethanesulfonic acid (triflic acid, TfOH) is reported to cleave Si–O–Si linkages of silsesquioxane cages under formation of bis(triflates), a reaction plausibly involving silanol intermediates.^[12,13] Despite reports on cage rearrangements during the acid-catalyzed hydrolysis of $T_7Ph_7(OH)_3$ and related incompletely condensed species,^[14] we speculated that TfOH may either substitute the Si–OH groups of the incompletely condensed $T_7Ph_7(OH)_3$ 1 or catalyze the condensation to $T_{14}Ph_{14}$.

In an initial attempt targeting the tris(triflate) $T_7Ph_7(OTf)_3$, three equivalents of TfOH were added to 1 in toluene at room temperature (Scheme 1). This resulted in a product mixture from which low amounts of a product with three ^{29}Si NMR signals at $\delta = -76.1$, -77.5 and -79.1 ppm in C_6D_6 were obtained by cooling a hot, concentrated toluene solution to room temperature. The absence of OH signals in the 1H NMR and of any ^{19}F NMR signal suggested that instead of substitution of OH by OTf condensation to a symmetrical $T_{14}Ph_{14}$ derivative had occurred. As in this case triflic acid would be needed in catalytic quantities only, we repeated the reaction with 10 mol% of TfOH and in the presence of molecular sieves (to capture the released water upon substitution) in toluene and indeed obtained the same product in 39% yield after evaporation of the volatiles and precipitation from minimal amounts of toluene.



Scheme 1. a) Synthesis of the D_{3h} - $T_{14}Ph_{14}$ isomer 2 from incompletely condensed silsesquioxane $Ph_7T_7(OH)_3$ 1 catalyzed by TfOH (●: silicon vertex). b) Treatment of $T_7Ph_7(OH)_3$ with 20 equivalents of triflic acid results in a minute quantity of $T_7Ph_7(OTf)_3$ among other non-isolated $T_7Ph_7(OTf)_n(OH)_{3-n}$ species.

Single crystals were grown by slowly cooling a concentrated toluene solution from approx. 100 °C to room temperature in the course of 16 h. An X-ray diffraction study (Figure 2)^[15] indeed confirmed the formation of the condensation product of two molecules of $T_7Ph_7(OH)_3$ 1 across the three silanol functions. The $T_{14}Ph_{14}$ cage 2 thus shows approximated D_{3h} symmetry with the three edge-sharing $(RSiO)_4$ rings of each T_7 unit connected by three $(RSiO)_6$ motifs ($6^35^04^6$; the base referring to the number of SiO units in a given ring motif and the exponent to the

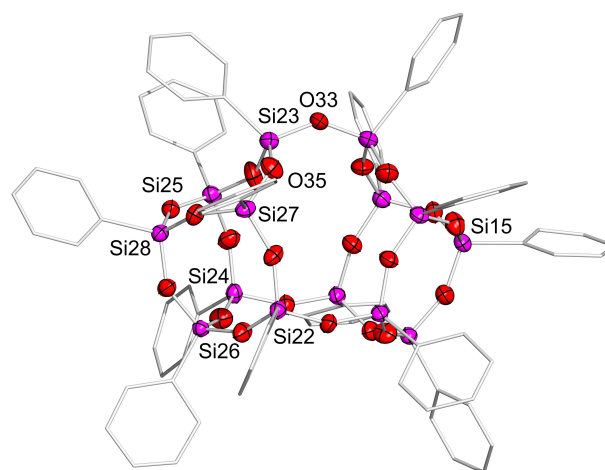


Figure 2. Molecular structure of $T_{14}Ph_{14}$ silsesquioxane 2 in the solid state. The idealized D_{3h} symmetry has no crystallographic correspondence. Thermal ellipsoids at 50% probability level, two of the three molecules in the asymmetric unit as well as hydrogen atoms and co-crystallized solvent molecules are omitted for clarity.

number of occurrences).^[4d] This connectivity is in marked contrast to the two crystallographically characterized isomers of the $T_{14}H_{14}$ parent species isolated by Agaskar et al. in a multiple step separation effort and with the very small combined yield of 1.1 %.^[4d] The D_{3h} - $T_{14}H_{14}$ isomer shows $6^05^64^3$ and its C_{2v} isomer $6^15^44^4$ connectivity. The $6^35^04^6$ isomer of $T_{14}H_{14}$ had been proposed to be part of the reaction mixture together with a fourth isomer of $6^25^24^5$ connectivity on the basis of GC-MS analysis, although no further information on its structure had been given in the absence of analytical data in solution and the solid state.^[4d] In subsequent computations on $T_{14}H_{14}$, however, only the two experimentally confirmed isomers plus the elusive $6^35^04^6$ motif reported in here as phenyl-substituted version **2** were considered^[16] revealing its strong energetic disadvantage by approximately $14.7 \text{ kcal mol}^{-1}$ at the MP2/SBK level of theory.^[16b]

The asymmetric unit of the crystals of **2** consists of three crystallographically independent molecules with noticeable differences in the bonding parameters although all show approximate D_{3h} symmetry. The silicon-oxygen bond lengths in the three molecules vary between $1.583(7) \text{ \AA}$ and $1.638(6) \text{ \AA}$ as opposed to the relatively uniform case of T_8Ph_8 (with Si–O bond lengths between 1.617 \AA and 1.626 \AA).^[17] In contrast, the OSiO bond angles are rather uniform and differ just slightly from T_8Ph_8 . The range of SiOSi bond angles in **2** ($T_{14}Ph_{14}(1)$: $138.8(4)^\circ$ to $172.0(6)^\circ$, $T_{14}Ph_{14}(2)$: $138.0(4)^\circ$ to $162.6(4)^\circ$ and $T_{14}Ph_{14}(3)$: $141.0(4)^\circ$ to $155.3(4)^\circ$) is larger than in T_8Ph_8 (142.28° to 153.22°) for all three independent molecules. Figure S14 shows superpositions of two molecules each in order to visualize the geometrical deviations (see Supporting Information).

The $T_{14}Ph_{14}$ silsesquioxane **2** gives rise to three signals in the ^{29}Si NMR at -76.2 , -77.6 and -79.1 ppm in C_6D_6 as depicted in Figure 3, which is in the usual range of phenyl-substituted silsesquioxanes.^[18] Compared to the $Ph_7T_7(OH)_3$ starting material (-68.3 , -76.9 and -77.8 ppm) the chemical shifts of **2** are closer together due to the very similar coordination environment at each silicon center. A 1H - ^{29}Si correlation NMR experiment in $CDCl_3$ (Figure S8) indicates the signal at -76.9 ppm to represent the two silicon atoms located on the C_3 rotation axis

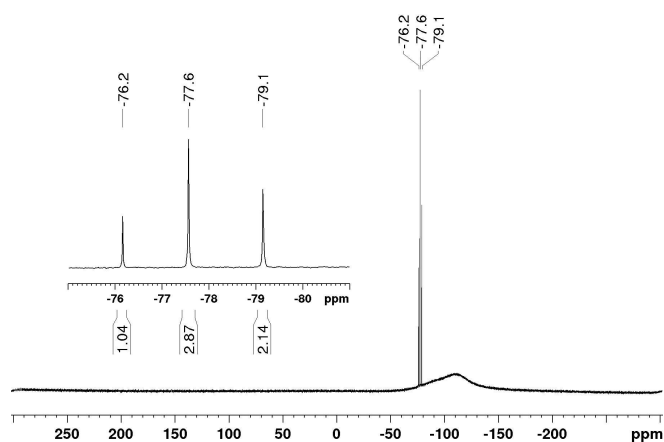


Figure 3. ^{29}Si NMR spectrum of the $T_{14}Ph_{14}$ silsesquioxane **2** in C_6D_6 at 25°C . The insert shows the signals with their relative intensities.

in the T_7 fragments (Si28 and Si15 atoms in Figure 2), by assignment of the corresponding ^1H NMR resonances to the *meta* hydrogen atoms of the phenyl groups based on the relative intensities (see Figures S1 and S2). The $^{29}\text{Si}/\text{CP}$ MAS spectrum of the crystalline material (Figure S7) shows an unresolved single broad peak at -77.8 ppm. The reported $T_{12}Ph_{12}$ $^{29}\text{Si}/\text{CP}$ MAS spectrum shows two well-resolved signals at -76.8 and -80.4 ppm,^[4e] in accordance with the two distinctly different chemical environments of the Si atoms. In our case, it is not surprising that the different silicon environments cannot be resolved in the solid state given the 42 silicon atoms of the three crystallographically inequivalent $T_{14}Ph_{14}$ molecules with only slightly different chemical environments. Diagnostically, the IR spectrum in Figure S10 of silsesquioxane **2** (ATR) lacks the distinct OH bands of the $T_7Ph_7(OH)_3$ precursor ($\nu_{\text{OH}} = 3234 \text{ cm}^{-1}$, $\nu_{\text{SiOH}} = 885 \text{ cm}^{-1}$, Figure S9)^[18] but is otherwise almost identical. Thermogravimetric analysis and differential scanning calorimetry of the $T_{14}Ph_{14}$ isomer show a behavior similar to that of the T_8Ph_8 to $T_{12}Ph_{12}$ systems (see Supporting Information for details).

DFT optimization of the four isomers in the $T_{14}Ph_{14}$ system at the B3LYP/6-311G level of theory (Figure 4) revealed the D_{3h} ($6^05^64^3$) (framework E in Figure 1) to be the most stable representative, while the herein synthesized D_{3h} ($6^35^04^6$) isomer **2** is the least stable at 13 kcal mol^{-1} . This reflects the previously reported findings for $T_{14}H_{14}$.^[16] The most stable D_{3h} isomer features the largest ratio of five-membered SiO rings to four- or six membered ones. This is in line with the observation that the five membered SiO ring systems are less strained and thus more stable.^[7,16b] As can be seen in Figure 4, the higher the number of four and six membered rings, the higher the relative energy of the $T_{14}Ph_{14}$ isomer. In contrast to the experimental

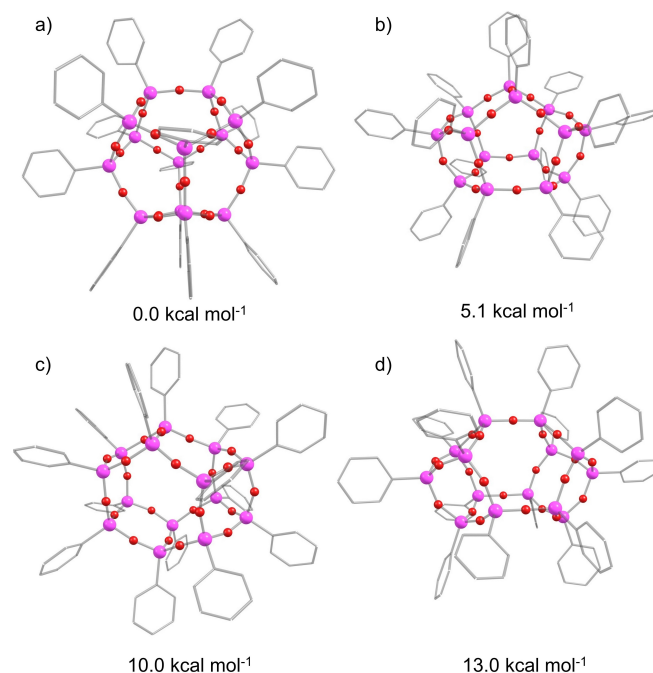


Figure 4. Optimized structures of the $T_{14}Ph_{14}$ isomers. a) D_{3h} ($6^05^64^3$) isomer, b) C_{2v} ($6^15^44^4$) isomer, c) C_{2v} isomer ($6^25^24^5$), d) D_{3h} ($6^35^04^6$) isomer.

solid state structure, the SiOSi bond angles are relatively uniform between 178.001° and 179.335° . Due to the well-established facile variation of the siloxane linkage, packing effects in the crystal lattice readily explain the deformation of the SiOSi angles in silsesquioxanes and can deviate by a large margin from calculations in the gas phase.^[3,19] The SiO bond lengths vary between 1.653 and 1.684 Å, which is overall slightly longer than in the experimental case as well-known for many DFT-functionals. In concert with the tendency of TfOH to cleave siloxane bonds under thermodynamic conditions, the high relative energy of the here reported D_{3h} ($6^35^46^6$) isomer suggests that silsesquioxane **2** represents the kinetic product of the reaction.

In order to broaden the scope of the systematic preparation of large silsesquioxanes, we attempted to isolate the incompletely condensed silsesquioxane as tris(triflate) derivative **3**, despite clear indications that it was unlikely to be an intermediate in the catalyzed formation of **2**. The reverse addition of the trisilanol **1** as suspension in toluene to a large extent of TfOH (20 eq) was expected to favor the stoichiometric reaction. Indeed, the biphasic mixture produced a small quantity of colorless single crystals after layering the separated toluene phase with hexane (Scheme 1). X-ray diffraction analysis revealed the heavily disordered structure of **3** (Figure 5), which may serve as strong indication for its formation but does not allow for the discussion of structural parameters. Unfortunately, the extreme sensitivity of **3** prevented a spectroscopic characterization of the minute amount obtained. In addition, as water is released during the substitution of OH by TfOH under the conditions described above, an unfavorable equilibrium reaction may complicate the isolation of **3** in larger quantities. The use of triflic anhydride Tf_2O instead of TfOH was expected to avoid this issue but did not produce satisfying results, as depending on the reaction conditions variable amounts of $T_{14}Ph_{14}$ along with unidentified byproducts at ambient temperatures or intractable product mixtures (between $-78^\circ C$ and $0^\circ C$) are obtained. Attempts to quench potential triflate species with suitable nucleophiles such as MeOH resulted in incon-

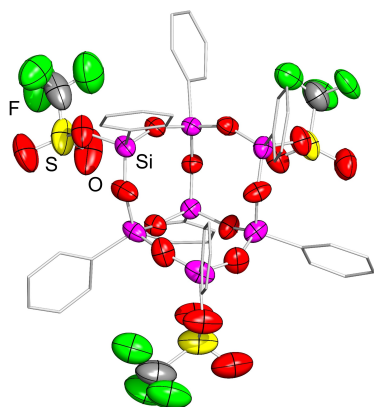


Figure 5. Highly disordered structure of silsesquioxanes tris(triflate) **3** in the solid state. Hydrogen atoms and disorder of phenyl and OTf groups are omitted for clarity. While the structure confirms the formation of the $T_7Ph_7(OH)_3$ species, the pronounced disorder of the OTf groups is prohibitive with regards to a discussion of bonding parameters.

clusive NMR spectra. Increasing the excess of triflic acid even further was not considered a viable option as it may favor competing side reactions such as ring opening and cage-rearrangements as reported by Feher and coworkers for other silsesquioxanes.^[20]

Based on above findings and considerations, it can be safely assumed that the mechanism of the condensation dimerization of **1** to the here reported D_{3h} -symmetric $T_{14}Ph_{14}$ isomer **2** does not involve intermediate tris(triflates) to any significant extent although they undoubtedly occur in low concentration under the reaction conditions. Instead we assume a catalytic cycle that closes the three required SiOSi linkages in a stepwise manner.

Conclusions

We conclude that whereas all hitherto reported polyhedral silsesquioxanes $(RSiO_{1.5})_n$ of cage sizes beyond $n = 8$ have been obtained as side-products of the smaller congeners in typically low yield and required complicated separation protocols, the here presented approach via an unprecedented catalytic condensation dimerization of $T_7Ph_7(OH)_3$ to give $T_{14}Ph_{14}$ is simple and straightforward. This allowed for the first complete characterization of a $T_{14}Ph_{14}$ silsesquioxane, a substituted representative of the elusive second D_{3h} isomer of $T_{14}H_{14}$. The high yielding and reproducible TfOH-catalyzed synthesis of the largest organically substituted polyhedral silsesquioxane from commercially available $Ph_7T_7(OH)_3$ opens the door to the development of an entirely new field of silsesquioxane chemistry. The reactivity of $T_{14}Ph_{14}$ is currently being investigated in our laboratory.

Experimental

General. All manipulations were conducted under a protective argon atmosphere using standard Schlenk techniques unless otherwise stated. Non-chlorinated solvents were dried over Na/benzophenone (in the presence of tetraglyme in case of aromatic and aliphatic solvents) and distilled under argon atmosphere. Deuterated solvents were dried by reflux over potassium and distilled under argon atmosphere prior to use. NMR spectra were recorded on either a Bruker Avance III 300 NMR spectrometer (1H : 300.13 MHz, ^{13}C : 75.46 MHz, ^{19}F : 282.4 MHz, ^{29}Si : 59.63 MHz) or a Bruker Avance III 400 spectrometer (1H : 400.12 MHz, ^{13}C : 100.61 MHz, ^{29}Si : 79.49 MHz) at 300 K. Thermogravimetric Analysis (TGA) was performed on a TGA/DSC Stare System 1 (Mettler-Toledo) and applying a heating rate of 10 K/min between 30 and 1000 °C. The Ar gas flow was set to 60 mL/min. Differential Scanning Calorimetry (DSC) was performed on a DSC 204 F1 Phoenix calorimeter (NETZSCH-Gerätebau GmbH) using an aluminum crucible with a pierced lid under nitrogen atmosphere (60 mL/min). A heating rate of 10 K/min from 25 to 415 °C was applied, with an isothermal step for 5 min at 415 °C. A cooling rate of 15 K/min from 415 °C to 25 °C was applied. Elemental analysis was carried out with an elemental analyzer Leco CHN-900. $T_7Ph_7(OH)_3$ was obtained from Hybrid Plastics, Inc. and dried under vacuum prior to use. Trifluoromethanesulfonic acid was obtained from TCI Belgium and distilled over a small amount of trifluoromethanesulfonic anhydride. Trifluoromethanesulfonic anhydride was obtained from Fluorochem and distilled over P_4O_{10} prior to use.

Preparation of T₁₄Ph₁₄ 2. A suspension of 1.27 g T₇Ph₇(OH)₃ in 13 mL of toluene is treated with 0.13 mL of a 1 M stock solution of freshly distilled trifluoromethanesulfonic acid in dichloromethane at room temperature in the presence of molecular sieve 4 Å. The reaction mixture is stirred for 30 minutes at ambient temperature, then for 15 minutes at 50 °C. The volatiles are evaporated under reduced pressure using a warm water bath. From here on, protective atmosphere or dry solvents are no longer necessary. The obtained residue is washed with another 2 mL of toluene at 0 °C. The product is again dissolved in 2 mL of dichloromethane and separated from the molecular sieves via filtration. 7 mL of toluene are used to separate the T₁₄Ph₁₄ from residual toluene-insoluble byproducts. Evaporation of toluene gives 475 mg of a white powder (39% yield). (m.p. 407 °C). ¹H NMR (400 MHz, C₆D₆, 300 K): 7.96–7.92 (m, 4H, *m*-Ph-H), 7.79–7.70 (m, 24H, *m*-Ph-H), 7.14–7.01 (m, 12H, *o*, *p*-Ph-H, overlapping with toluene-H), 6.97–6.93 (m, 18H, *o*, *p*-Ar-H), 6.86–6.82 (m, 12H, *o*, *p*-Ph-H) ppm. ¹H NMR (400 MHz, CDCl₃, 300 K): 7.76–7.74 (m, 4H, *m*-Ph-H), 7.56–7.54 (m, 12H, *m*-Ph-H), 7.47–7.44 (m, 12H, *m*-Ph-H), 7.38–7.33 (m, 10H, *o*, *p*-Ph-H), 7.27–7.20 (m, 20H, *o*, *p*-Ph-H, overlapping with toluene-H), 7.10–7.06 (m, 12H, *o*, *p*-Ph-H) ppm. ¹³C NMR (100 MHz, C₆D₆, 300 K): 134.6, 134.5, 132.0, 131.3, 131.1, 130.9, 130.7, 130.5, 129.3, 128.6, 128.5, 128.2, 125.7 (each Ph-C) ppm. ¹³C NMR (100 MHz, CDCl₃, 300 K): 134.3, 134.2, 134.1, 131.7, 131.2, 130.9, 130.8, 130.4, 130.2, 128.1, 127.8, 127.7 (each Ph-C) ppm. ²⁹Si NMR (79.5 MHz, C₆D₆, 300 K): –76.2, –77.6, –79.1 ppm. ²⁹Si NMR (79.5 MHz, CDCl₃, 300 K): –76.9, –78.3, –80.1 ppm. CP-MAS-²⁹Si NMR: (79.5 MHz, 13 kHz, 300 K) –77.8 ppm. **Elemental Analysis:** Calc. for C₈₄H₇₀O₂₁Si₁₄: C, 55.78; H, 3.90; Found: C, 56.11; H, 3.86.

Supporting Information

Plots of NMR and IR spectra as well as details of thermal analysis, X-ray structures and DFT calculations. The authors have cited additional references within the Supporting Information.^[21–28]

Acknowledgements

We gratefully acknowledge the funding by Saarland University. We acknowledge the Service Center X-ray Diffraction established with financial support from Saarland University and the Deutsche Forschungsgemeinschaft (INST 256/506-1). We thank Svenja Pohl, Jan-Falk Kannengießner and Elias Gießelmann for the TGA, DSC and solid state NMR measurements. Open Access funding enabled and organized by Projekt DEAL.

Conflict of Interests

The authors declare no conflict of interest.

Data Availability Statement

The data that support the findings of this study are available in the supplementary material of this article.

Keywords: Cage structures · Reactive Intermediates · silsesquioxanes · silyl triflates

- a) S. M. Ramirez, Y. J. Diaz, C. M. Sahagun, M. W. Duff, O. B. Lawal, S. T. Ianoco, J. M. Mabry, *Polym. Chem.* **2013**, *4*, 2230–2234; b) R. J. Clark, M. Aghajamali, C. M. Gonzalez, L. Hadidi, M. A. Islam, M. Javadi, M. H. Mobarok, T. K. Purkait, C. J. T. Robidillo, R. Sinelnikov, A. N. Thiessen, J. Washington, H. Yu, J. C. C. Veinot, *Chem. Mater.* **2017**, *29*, 80–89; c) J. Shen, F. Aydinoglu, M. Soltani, B. Cui, *J. Vac. Sci. Technol. B* **2019**, *37*, 021601; d) M. Gon, K. Tanaka, Y. Chujo, *Chem. Asian J.* **2022**, *17*, e2202200144.
- F. J. Feher, D. A. Newman, J. F. Walzer, *J. Am. Chem. Soc.* **1989**, *111*, 1741–1748.
- D. B. Cordes, P. D. Lickiss, F. Rataboul, *Chem. Rev.* **2010**, *110*, 2081–2173.
- a) A. J. Barry, W. H. Daudt, J. J. Domicone, J. W. Gilkey, *J. Am. Chem. Soc.* **1955**, *77*, 4248–4252; b) J. F. Brown, L. H. Vogt, *J. Am. Chem. Soc.* **1965**, *87*, 4313–4317; c) P. A. Agaskar, V. W. Day, W. G. Klemperer, *J. Am. Chem. Soc.* **1987**, *109*, 5554–5556; d) P. A. Agaskar, W. G. Klemperer, *Inorg. Chim. Acta* **1995**, *229*, 355–364; e) A. R. Bassindale, Z. Liu, I. A. MacKinnon, P. G. Taylor, Y. Yang, M. E. Light, P. N. Horton, M. B. Hursthouse, *Dalton Trans.* **2003**, 2945–2949.
- a) D. Hossain, C. U. Pittman, S. Saebø, F. Hagelberg, *J. Phys. Chem. C* **2007**, *111*, 6199–6206; b) M. Z. Asuncion, R. M. Laine, *J. Am. Chem. Soc.* **2010**, *132*, 3723–3736; c) S. Chimjarn, R. Kunthom, P. Chancharone, R. Sodkhomkhum, P. Sangtrirutnugul, V. Ervithayasuporn, *Dalton Trans.* **2015**, *44*, 916–919; d) K. Imai, Y. Kaneko, *Inorg. Chem.* **2017**, *56*, 4133–4140.
- Y. Kawakami, K. Yamaguchi, T. Yokozawa, T. Serizawa, M. Hasegawa, Y. Kabe, *Chem. Lett.* **2007**, *36*, 792–793.
- M. Laird, N. Hermann, N. Ramsahye, C. Totée, C. Carcel, M. Unno, J. R. Bartlett, M. Wong Chi Man, *Angew. Chem.* **2021**, *133*, 3059–3064; *Angew. Chem. Int. Ed.* **2021**, *60*, 3022–3027.
- a) X. Lin, Y.-Y. Deng, Q. Zhang, D. Han, Q. Fu, *Macromolecules* **2023**, *56*, 1243–1252; b) J. Wang, X. Lin, D.-L. Zhou, S.-R. Fu, Q. Zhang, H. Bai, D. Han, Q. Fu, *Macromol. Mater. Eng.* **2023**, *308*, 2300076.
- S. Spirk, M. Nieger, F. Belaj, R. Pietschnig, *Dalton Trans.* **2009**, 163–167.
- D. Brzakałski, R. E. Przekop, B. Sztorch, P. Jakubowska, M. Jałbrzykowski, B. Marciniak, *Polymer* **2020**, *12*, 2269.
- N. Hurkes, C. Bruhn, F. Belaj, R. Pietschnig, *Organometallics* **2014**, *33*, 7299–7306.
- F. J. Feher, F. Nguyen, D. Soulivong, J. W. Ziller, *Chem. Commun.* **1999**, 1705–1706.
- F. J. Feher, D. Soulivong, A. G. Eklund, *Chem. Commun.* **1998**, 399–400.
- J. C. Furgal, T. Goodson III, R. M. Laine, *Dalton Trans.* **2016**, *45*, 1025–1039.
- Deposition numbers 2300495 (for 2) and 2300496 (for 3) contain the supplementary crystallographic data for this paper. These data are provided free of charge by the joint Cambridge Crystallographic Data Centre and Fachinformationszentrum Karlsruhe Access Structures service.
- a) K.-H. Xiang, R. Pandey, U. C. Pernisz, C. Freeman, *J. Phys. Chem. B* **1998**, *102*, 8704–8711; b) T. Kudo, *J. Phys. Chem. A* **2009**, *113*, 12311–12321.
- P. R. Chinnam, M. R. Gau, J. Schwab, M. J. Zdilla, S. L. Wunder, *Acta Crystallogr. Sect. C* **2014**, *70*, 971–974.
- Y. Sato, R. Hayami, T. Gunji, *J. Sol-Gel Sci. Technol.* **2022**, *104*, 36–52.
- A. R. Bassindale, H. Chen, Z. Liu, I. A. MacKinnon, D. J. Parker, P. G. Taylor, Y. Yang, M. E. Light, P. N. Horton, M. B. Hursthouse, *J. Organomet. Chem.* **2004**, *689*, 3287–3300.
- F. J. Feher, D. Soulivong, F. Nguyen, *Chem. Commun.* **1998**, 1279–1280.
- C. Pakjamsai, Y. Kawakami, *Des. Monomers Polym.* **2005**, *8*, 423–435.
- P. J. Jones, R. D. Cook, C. N. McWright, R. J. Nalty, V. Choudhary, S. E. Morgan, *Appl. Polym. Sci.* **2011**, *121*, 2945–2956.
- G. M. Sheldrick, *Acta Crystallogr.* **2015**, *A71*, 3–8.
- G. M. Sheldrick, *Acta Crystallogr.* **2015**, *C71*, 3–8.
- C. B. Hübschle, G. M. Sheldrick, B. Dittrich, *J. Appl. Crystallogr.* **2011**, *44*, 1281–1284.
- Gaussian 16, Revision C.01, M. J. Frisch, G. W. Trucks, H. B. Schlegel, G. E. Scuseria, M. A. Robb, J. R. Cheeseman, G. Scalmani, V. Barone, G. A. Petersson, H. Nakatsuji, X. Li, M. Caricato, A. V. Marenich, J. Bloino, B. G. Janesko, R. Gomperts, B. Mennucci, H. P. Hratchian, J. V. Ortiz, A. F. Izmaylov, J. L. Sonnenberg, D. Williams-Young, F. Ding, F. Lipparini, F. Egidi, J. Goings, B. Peng, A. Petrone, T. Henderson, D. Ranasinghe, V. G. Zakrzewski, J. Gao, N. Rega, G. Zheng, W. Liang, M. Hada, M. Ehara, K.

- Toyota, R. Fukuda, J. Hasegawa, M. Ishida, T. Nakajima, Y. Honda, O. Kitao, H. Nakai, T. Vreven, K. Throssell, J. A. Montgomery, Jr., J. E. Peralta, F. Ogliaro, M. J. Bearpark, J. J. Heyd, E. N. Brothers, K. N. Kudin, V. N. Staroverov, T. A. Keith, R. Kobayashi, J. Normand, K. Raghavachari, A. P. Rendell, J. C. Burant, S. S. Iyengar, J. Tomasi, M. Cossi, J. M. Millam, M. Klene, C. Adamo, R. Cammi, J. W. Ochterski, R. L. Martin, K. Morokuma, O. Farkas, J. B. Foresman, and D. J. Fox, Gaussian, Inc., Wallingford CT, 2019.
- [27] a) A. D. Becke, *J. Chem. Phys.* **1993**, *98*, 5648–5652; b) C. Lee, W. Yang, R. G. Parr, *Phys. Rev. B* **1988**, *37*, 785–789; c) A. D. Becke, *Phys. Rev. A* **1988**, *38*, 3098–3100.
- [28] a) R. Krishnan, J. S. Binkley, R. Seeger, J. A. Pople, *J. Chem. Phys.* **1980**, *72*, 650–654; b) A. D. McLean, G. S. Chandler, *J. Chem. Phys.* **1980**, *72*, 5639–5648.

Manuscript received: November 2, 2023

Accepted manuscript online: December 6, 2023

Version of record online: January 26, 2024